

An SYK-Like Model Without Disorder

Edward Witten

*School of Natural Sciences, Institute for Advanced Study
Einstein Drive, Princeton, NJ 08540 USA*

Abstract

Making use of known facts about “tensor models,” it is possible to construct a quantum system without quenched disorder that has the same large n limit for its correlation functions and thermodynamics as the SYK model. This might be useful in further probes of this approach to holographic duality.

1 Introduction

The SYK model [1, 2] is a quantum mechanical model of fermions with random couplings. The most widely studied version of the model has N real fermions ψ_i , $i = 1, \dots, N$, with q -fold random couplings, for some even integer $q \geq 4$. The model can be described by the action

$$I = \int dt \left(\frac{i}{2} \sum_i \psi_i \frac{d}{dt} \psi_i - i^{q/2} j_{i_1 i_2 \dots i_q} \psi_{i_1} \psi_{i_2} \dots \psi_{i_q} \right). \quad (1.1)$$

Here the couplings are Gaussian random variables. If we write I for a multi-index $i_1 i_2 \dots i_q$, the j_I are drawn from a Gaussian ensemble with variance

$$\langle j_I j_{I'} \rangle = \delta_{II'} \frac{J^2 (q-1)!}{N^{q-1}}, \quad (1.2)$$

for some constant J .

The model is solvable in the limit of large N , fixed J by a saddle point method that reflects the fact that the dominant Feynman diagrams in this limit have a simple type. They can be generated by an iterative procedure that is illustrated in fig. 1. At each stage of the iteration, one takes a propagator (fig 1(a)) and replaces it by the diagram of fig. 1(b). This can be done any number of times to generate more complicated diagrams. For example, at the second step of the iteration, one can generate the diagram of fig. 1(c).

A model of this general type was formulated many years ago [1] to describe a spin-fluid state, but the subject has attracted renewed interest because of the suggestion [2] that the large N limit of the model is dual to a black hole in an emergent 1+1-dimensional spacetime. This type of model was first discussed in relation to holographic duality in [3]. For recent work, see [4–18].

One question that one might ask about the SYK model is whether, instead of formulating it as a model with quenched disorder, one can find similar physics in a more conventional large N limit. One idea might be to interpret the couplings j_I as quantum variables with very slow dynamics, rather than random constants. Even if it works, this has the drawback that the thermodynamic entropy of the j_I (roughly $N^q/q!$ bosonic variables) will overwhelm that of the ψ_i (N fermionic variables).

The present paper is devoted to another approach that does not have this drawback. In fact, there is an already known class of “tensor models” whose large N limits are governed by precisely the same Feynman diagrams that dominate the large N limit of the SYK model. There have been many papers on this subject, a sampling being [19–26]. In this literature, the dominant graphs are called “melons” or “melonic graphs.” A convenient reference is [22]. The construction of tensor models was motivated by the idea of generalizing to higher dimensions the familiar relation of matrix models to random two-dimensional geometries.¹ In that application, the dimension D is

¹This idea also motivated an earlier literature on more generic tensor models that do not necessarily have a large N limit similar to that of the SYK model. See for example [27–29].



Figure 1: The iterative procedure that generates the leading diagrams of the SYK model for large N . Figures are drawn for $q = 4$ (quartic vertices). At each step of the process, one replaces a propagator (part (a)) with the two-loop diagram of part (b). For example, after another iteration, one can generate the four-loop diagram of part (c).

related to the order q of the SYK interactions by $D = q - 1$. The status of this program is unclear, since it is not clear that the rather special Feynman diagrams that are generated by the procedure summarized in fig. 1 describe a useful class of random D -geometries. But because the tensor models are governed in the large N limit by the same Feynman diagrams as the SYK model, they do give a framework to eliminate the quenched disorder of the SYK model in favor of a more standard large N limit.

It is not entirely clear that this is helpful, but there are at least two reasons that it might be. First, the average of a quantum system over quenched disorder is not really a quantum system, so the reliance on quenched disorder might make it difficult to apply the SYK model to some subtle questions about black holes. Second, in the SYK model, certain bilinear expressions in the ψ_i , which roughly speaking are “singlets” in a disorder-averaged sense, appear to have natural duals in the emergent two-dimensional world. But it is not clear that the N fields ψ_i themselves have a natural interpretation of that sort. At any rate, their analogs do not have bulk duals in better-understood examples of gauge/gravity duality. The tensor models that mimic the SYK model can be chosen, as we will do in section 2, to have a global symmetry group G whose dimension is relatively large, but still much less than N . Gauging the G symmetry leaves as gauge-invariant operators the singlet operators that are relevant in the gravitational dual description, but eliminates the elementary fermion fields themselves. But because the dimension of G is much less than N , gauging the symmetry does not significantly affect the thermodynamics of the model when N is large.

In section 2, we describe a variant of the SYK model that has a similar large N limit but without quenched disorder. In doing this, we adapt and modify the construction described in [22] (and other papers cited above) in minor ways. Our fields are fermion fields in $0 + 1$ spacetime dimensions rather than boson fields in 0 dimensions. Also, we construct a simple model with a relatively large amount of symmetry (which could be gauged) and do not discuss some of the more generic models that have been considered in the literature. None of this affects the counting of powers of N in Feynman diagrams. As in [2] and many subsequent papers, we use real fermion fields. As a result, the index loops we encounter are unoriented and certain two-manifolds that arise may be unorientable. We could instead use complex fermion fields as in [1]; then as in [22],

the index loops and two-manifolds will be oriented.

In section 3, following [22], we sketch the proof that the Feynman diagrams that survive in the large N limit of the tensor model are precisely those of the SYK model. The $1/N$ corrections are different, though the significance of the difference is not clear.

2 The Model

The model will be constructed with $q = D + 1$ real fermion fields ψ_0, \dots, ψ_D . Each will have n^D real components, for some integer n , so the total number of real fermion fields will be $N = (D + 1)n^D$.

For each a , the field ψ_a will transform in a real irreducible representation of a symmetry group G , as follows. First of all, for each unordered pair a, b of distinct elements of the finite set $\{0, 1, \dots, D\}$, we introduce a copy G_{ab} of the group $O(n)$. Since the pair a, b is unordered, we do not distinguish G_{ab} from G_{ba} . The full symmetry group of the model is then a product

$$G_0 = \prod_{a < b} G_{ab} \cong O(n)^{D(D+1)/2}, \quad (2.1)$$

up to a discrete quotient that we consider in a moment.

For each a , we now declare that ψ_a transforms as the tensor product of the vector representations of G_{ab} for every $b \neq a$, and transforms trivially under G_{bc} if $b, c \neq a$. The vector representation of G_{ab} is n -dimensional, and there are D groups G_{ab} with $b \neq a$, so ψ_a has n^D real components, as stated above. With this choice for the fermion representation, a certain discrete subgroup of G_0 acts trivially. The center of $O(n)$ is \mathbb{Z}_2 , acting by sign change on the vector representation, so the center of G_0 is $\mathbb{Z}_2^{D(D+1)/2}$. A certain subgroup $\mathbb{Z}_2^{(D-2)(D+1)/2}$ acts trivially on all the ψ_a , so the group that will be a faithfully acting symmetry group of the theory is

$$G = G_0 / \mathbb{Z}_2^{(D-2)(D+1)/2}. \quad (2.2)$$

We now replace the SYK action with

$$I = \int dt \left(\frac{i}{2} \sum_i \psi_i \frac{d}{dt} \psi_i - i^{q/2} j \psi_0 \psi_1 \dots \psi_D \right), \quad (2.3)$$

with a real coupling parameter j . The meaning of the expression $\psi_0 \psi_1 \dots \psi_D$ is as follows. For each $a < b$, precisely two of these fields, namely ψ_a and ψ_b , transform as vectors under G_{ab} . Contracting the vector indices of G_{ab} for each pair a, b , we arrive at a G -invariant that we denote for brevity as $\psi_0 \psi_1 \dots \psi_D$.

Note that the Hamiltonian of the theory is $H = i^{q/2} j \psi_0 \psi_1 \dots \psi_D$. This Hamiltonian is odd under a *unitary* transformation that changes the sign of one of the ψ_a . (For a discussion of Hamiltonians

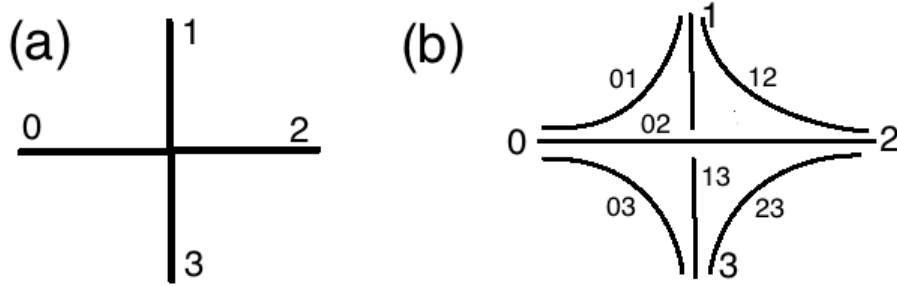


Figure 2: Two views of the basic Feynman vertex of the theory. Here and later, figures are drawn for quartic vertices ($q = 4$ or $D = 3$). In (a), the vertex is drawn as a simple quartic vertex with external lines labeled 0, 1, 2, or 3. In (b), each line is resolved into three “strands,” representing how the “indices” of a field transform under a symmetry group. For example, the field ψ_0 is a trifundamental of $G_{01} \times G_{02} \times G_{03}$, so it is represented with three strands labeled 01, 02, and 03. The vertex is constructed by connecting these strands in the only way consistent with their labeling. It can be visualized as a tetrahedron.

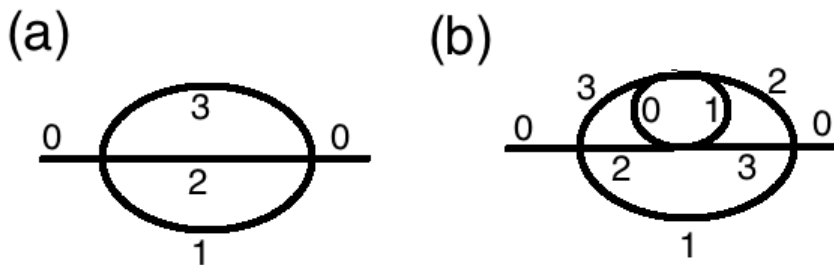


Figure 3: A typical diagram that survives (a) or does not survive (b) in the large n limit.

with the unusual property of being odd under a unitary symmetry, see [30].) It is observed in [10] that the Hamiltonian of the SYK model has this property on a statistical basis. Permutations of the ψ_a accompanied by corresponding permutations of the G_{ab} are global symmetries (an odd permutation must be accompanied by a sign change of one of the ψ_a).

Now we describe some basic properties of Feynman diagrams of this theory. In fig. 3, we depict in two different ways the basic Feynman vertex of the theory for $D = 3$ or $q = 4$. In part (a), it is simply shown as a basic quartic vertex for four fields $\psi_0, \psi_1, \psi_2,$ and ψ_3 . Propagation of one of these fields is represented as usual by a “line” in the Feynman graph. In part (b), we take note of the fact that each of the ψ_a is a trifundamental of a certain product of three copies of $O(n)$, and so can be considered to carry three n -valued “indices.” Accordingly, we resolve each “line” in part (a) into three “strands” in part (b). For example, a line of type 0 is resolved into strands of type 01, 02, and 03, reflecting the fact that ψ_0 transforms as a trifundamental of $G_{01} \times G_{02} \times G_{03}$. Then to construct the Feynman vertex, we connect all of the strands in the only way consistent with their labeling, arriving at the figure.

Hopefully the reader can visualize fig. 2(b) as representing a tetrahedron, with each vertex

labeled by an index $a \in \{0, 1, 2, 3\}$ and the edge connecting vertices a and b labeled as ab . This interpretation of the vertex as a tetrahedron is part of the relationship of the tensor models described in [19–26] (for $D = 3$) with three-geometries. For larger D , the tetrahedron is replaced by a D -simplex and the graphs can be interpreted as D -geometries. However, as noted in the introduction, the dominant Feynman diagrams, for large n , correspond to a fairly special class of D -geometries. The relation to the SYK model gives an alternative motivation to consider this class of model.

Now we make some preliminary remarks on the large n limit, or equivalently the large N limit. To count powers of n in a Feynman diagram, it is very convenient to think about the fact that each line in the diagram represents D strands, as in fig. 2(b). The strands can form closed loops and, as in the more familiar matrix models, such a closed loop gives a factor of n . A difference from matrix models is that there are different kinds of closed loops. A strand may be of type ab for any unordered pair $a, b \in \{0, 1, \dots, D\}$ and hence there are altogether $D(D + 1)/2$ distinct kinds of strand. We let \mathcal{F}_{ab} be the number of closed loops made of strands of type ab , and

$$\mathcal{F} = \sum_{a < b} \mathcal{F}_{ab}. \quad (2.4)$$

In [22], \mathcal{F}_{ab} is called the number of faces of type ab and \mathcal{F} the total number of faces. (The rationale for this terminology is that if one glues in a disc whose boundary is a closed strand of type ab , one gets a two-dimensional “face” of some triangulated geometry.) Summing over index loops will give a factor of

$$n^{\mathcal{F}} = \prod_{a < b} n^{\mathcal{F}_{ab}}. \quad (2.5)$$

Let us work this out in some simple examples. Some simple Feynman diagrams for $D = 3$ are drawn in fig. 3. The diagrams are drawn in the standard way, representing the propagation of one of the ψ_a by a line and not resolving the lines into strands. The reason is that diagrams soon become rather complicated if drawn in terms of strands. With a little practice, one can easily count powers of n without drawing the strands. Every closed loop in the graph that only contains lines of type a or b will, when resolved in strands, give a closed strand of type ab . This is the only source of closed strands of this type, so \mathcal{F}_{ab} is just the number of closed loops that can be drawn in the graph using only lines labeled a or b . We call these loops of type ab . (Loops of type ab are always disjoint, because of the form of the interaction vertex.) For example, in fig. 3(a) one can form a single closed loop of type 12, 13, or 23, and none of type $0a$ for any a . So for this diagram, $\mathcal{F} = \sum_{ab} \mathcal{F}_{ab} = 3$. Thus the diagram is proportional to $j^2 n^3$. So to ensure a large n limit, we must take

$$j = \frac{J}{n^{3/2}} \quad (2.6)$$

for some constant J .

Once we scale the coupling with n so that fig. 3(a) has a large n limit, it is almost immediate that any diagram made by the iterative procedure of fig. 1 likewise has a large n limit. However, other diagrams vanish for large n . Postponing a systematic explanation for section 3, we first examine in fig. 3(b) a simple diagram that is not generated by the iterative procedure. This diagram has one closed loop of type 01, one of type 23, one of type 12, and one of type 13. With

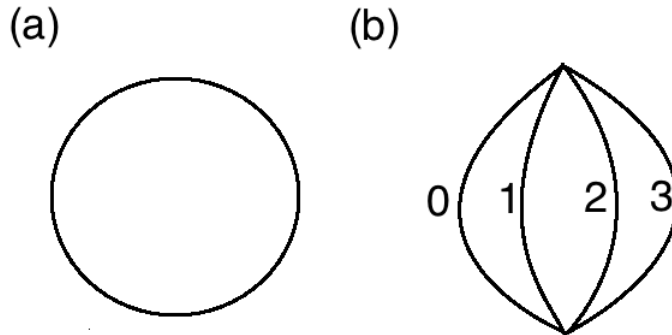


Figure 4: (a) The vacuum amplitude in free fermion theory is represented by this one-loop diagram (the loop may carry any label 0,1,2, or 3). (b) The lowest order nontrivial contribution to the vacuum amplitude, obtained by applying the iterative step in fig. 1 to the one-loop diagram in (a).

four vertices, this diagram is of order $j^4 n^4 \sim 1/n^2 \sim 1/N^{2/3}$. Thus the diagram is subleading in the large n or equivalently the large N limit. However, the $1/n$ corrections are different in this model from what they are in the SYK model, as the expansion in that model is an expansion in integer powers of $1/N$.

The examples we have considered were contributions to the two-point function. In a similar way, we can consider vacuum diagrams. In free field theory, we would just have the one-loop diagram of fig. 4(a). With N fermion fields, it makes a contribution of order N . Applying once the usual iterative step of fig. 1, we get the first nontrivial contribution to the vacuum amplitude in fig. 4(b). It is of order $j^2 n^6 = J^2 N$ and thus is again of order N for large N . Another iterative step can lead, for example, to the diagram of fig. 5, which is of order $j^4 n^9 = J^4 N$. In general, the leading contributions to the vacuum amplitude are generated by the iterative procedure and are of order N .

3 Some Details

Following [22], we will explain how to analyze the large n behavior of the perturbative expansion in a model of this kind. (We describe only the leading behavior. It is not clear how difficult it is to systematically describe the diagrams that arise in each order in $1/n$.)

It does not matter very much whether we study the large n limit for vacuum diagrams or for correlation functions, since leading order contributions to the $2k$ -point function are made by “cutting” k lines in a diagram that makes a leading order contribution to the vacuum amplitude. Thus, to understand the large n behavior of the perturbation expansion, it essentially suffices to

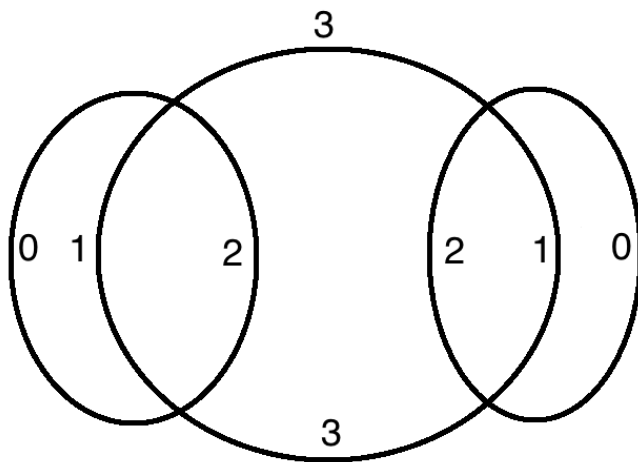


Figure 5: The next step in the iteration can generate this more complicated vacuum diagram, which also survives in the large N limit.

consider the vacuum amplitude. This will give a minor simplification in the following.

Let $\mathcal{J} = (a_0, a_1, \dots, a_D)$ be an unoriented cyclic ordering of the set $\{0, 1, \dots, D\}$; the term “unoriented” means that two cyclic orderings that differ by a mirror reflection are considered equivalent. Given such a \mathcal{J} , we can reduce any Feynman graph \mathcal{G} , such as the graph of fig. 5, to the graph of a more familiar matrix model, as follows. Each line in \mathcal{G} of type a_i (for some i) can be resolved in strands of type $a_i b$ for all $b \neq a_i$, making D strands in all. In the abstract, there is no natural way to pick just 2 of the strands associated to a given line. However, once we are given the cyclic arrangement $\mathcal{J} = (a_0, a_1, \dots, a_D)$, each label a_i has the two “neighbors” a_{i+1} and a_{i-1} . For each line of type a_i , we remember only the two strands of type $a_i a_{i\pm 1}$ and forget the others. When in this way we keep only two strands for each graph line in the graph, the lines we keep always meet smoothly at vertices and \mathcal{G} becomes a ribbon graph or fatgraph of a matrix model. (This will be a matrix model with unoriented index loops, as our fields are real and the individual strands are unoriented.) In the fashion familiar from matrix models, by gluing in discs whose boundaries are the closed index loops of type $a_i a_{i+1}$ (for all i), we make a closed two-manifold that we will call $\Sigma_{\mathcal{J}}$, since it depends on \mathcal{J} .

An important fact will be that the Euler characteristic of $\Sigma_{\mathcal{J}}$, which we denote $\chi_{\mathcal{J}}$, can be no larger than 2. We denote it as

$$\chi_{\mathcal{J}} = 2 - 2g_{\mathcal{J}}, \quad (3.1)$$

but we note that as our fields are real, $\Sigma_{\mathcal{J}}$ may be unorientable, so $\chi_{\mathcal{J}}$ may be odd and $g_{\mathcal{J}}$ defined this way may be a half-integer. At any rate, the important property is that $g_{\mathcal{J}}$ is nonnegative. Following [22], we define the “degree” of the graph \mathcal{G} as

$$\omega(\mathcal{G}) = \sum_{\mathcal{J}} g_{\mathcal{J}} = \sum_{\mathcal{J}} \left(1 - \frac{\chi_{\mathcal{J}}}{2}\right). \quad (3.2)$$

Thus $\omega(\mathcal{G}) \geq 0$ for all \mathcal{G} , and if $\omega(\mathcal{G}) = 0$ then $g_{\mathcal{J}} = 0$ for all \mathcal{J} , which means that the $\Sigma_{\mathcal{J}}$ are all two-spheres.

As an example of the definition of $g_{\mathcal{J}}$, we consider the diagram of fig. 5 and take $\mathcal{J} = (0, 1, 2, 3)$. This means that we are supposed to keep strands of type $ii + 1$ for any i . The planar diagram made this way is simply the obvious planar diagram associated with the fact that the graph of fig. 5 has been drawn in a plane. $\Sigma_{\mathcal{J}}$ is a two-sphere, constructed by adding a point at infinity to the plane in which the diagram has been drawn.

Let v_0 and v_1 be the number of vertices and edges in the graph \mathcal{G} . These do not depend on the choice of \mathcal{J} . However, the number of faces (discs that are glued in when we construct $\Sigma_{\mathcal{J}}$) does depend on \mathcal{J} . We denote this number as $v_{2,\mathcal{J}}$. It is

$$v_{2,\mathcal{J}} = \sum_{i=0}^D \mathcal{F}_{a_i a_{i+1}}, \quad (3.3)$$

since the faces of $\Sigma_{\mathcal{J}}$ are associated to index loops of type $a_i a_{i+1}$ (for some i). We also have $v_1 = \frac{D+1}{2} v_0$, because \mathcal{G} is constructed from $(D+1)$ -valent vertices.

The Euler characteristic of $\Sigma_{\mathcal{J}}$ is

$$\chi_{\mathcal{J}} = v_0 - v_1 + v_{2,\mathcal{J}} = - \left(\frac{D-1}{2} \right) v_0 + \sum_i \mathcal{F}_{a_i a_{i+1}}. \quad (3.4)$$

From this formula and (3.2), we can work out a useful formula for $\omega(\mathcal{G})$:

$$\frac{2}{(D-1)!} \omega(\mathcal{G}) = D + \frac{D(D-1)}{4} v_0 - \mathcal{F}. \quad (3.5)$$

The main point in the derivation is that each pair ab are adjacent in precisely $(D-1)!$ of the orderings \mathcal{J} and hence each \mathcal{F}_{ab} occurs $(D-1)!$ times when eqn. (3.4) is summed over \mathcal{J} .

Now we define the large n limit by taking

$$j = \frac{J}{n^{D(D-1)/4}} \quad (3.6)$$

with fixed J . A Feynman graph \mathcal{G} with v_0 vertices and \mathcal{F} closed strands (of any type ab) will be proportional then to

$$n^{-(D(D-1)/4)v_0 + \mathcal{F}} = n^{D-2\omega(\mathcal{G})/(D-1)!} = N^{1-2\omega(\mathcal{G})/D!}. \quad (3.7)$$

Since $\omega_{\mathcal{G}} \geq 0$ for all \mathcal{G} , the large N limit of any graph is at most proportional to N , and the graphs that do make contributions of order N are precisely those – such as that of fig. 5 – with $\omega_{\mathcal{G}} = 0$.

It remains then to understand which graphs do have $\omega_{\mathcal{G}} = 0$. The basic statement here (Lemma 1 in [22]) is that any graph with $\omega_{\mathcal{G}} = 0$ has a face of some type ab with only two vertices (in

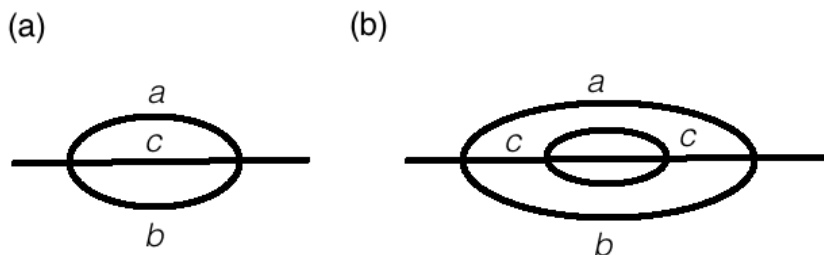


Figure 6: If \mathcal{G} has degree 0 and a face \mathcal{F}_* of type ab with only two faces, then a planar diagram of any type $(\dots acb\dots)$ looks near \mathcal{F}_* like (a) or (b). In (a), the two vertices of \mathcal{F}_* are connected by a single line labeled c and in (b) this line is replaced by a more complicated graph such as the one shown.

other words, some strand of type ab forms a closed loop after passing through only two vertices; for example, in fig. 5 there are two strands of type 01, two of type 02, and two of type 12 with this property). The proof in [22] is as follows.

If $\omega_{\mathcal{G}} = 0$, by definition this means that the total number of faces is $\mathcal{F} = \frac{D(D-1)}{4}v_0 + D$. Given the structure of the interaction vertex $\psi_0\psi_1\dots\psi_D$, in which each field appears only once, each closed strand must pass through an even number of vertices. Write \mathcal{F}_s for the number of faces with $2s$ vertices, so

$$\mathcal{F}_1 + \mathcal{F}_2 + \sum_{s>2} \mathcal{F}_s = \mathcal{F} = \frac{D(D-1)}{4}v_0 + D. \quad (3.8)$$

Let $2p_{\rho}^{ab}$ be the number of vertices of the ρ^{th} closed strand (or face) of type ab . One-half the total number of vertices of any face is

$$\sum_{\rho, a<b} p_{\rho}^{a,b} = \mathcal{F}_1 + 2\mathcal{F}_2 + \sum_{s>2} s\mathcal{F}_s. \quad (3.9)$$

Each vertex contributes to $D(D+1)/2$ faces of some type, so $\sum_{\rho, a<b} p_{\rho}^{a,b} = D(D+1)v_0/4$. Combining these formulass and eliminating \mathcal{F}_2 , we get

$$\mathcal{F}_1 = 2D + \sum_{s\geq 3} (s-2)\mathcal{F}_s + \frac{D(D-3)}{4}v_0. \quad (3.10)$$

Thus $\mathcal{F}_1 > 0$ for $D \geq 3$. For the SYK model, one has $q \geq 4$ and thus automatically $D = q - 1$ is ≥ 3 . (However, there are variants of the SYK model derived from random cubic tensors [16], and it is not immediately apparent how to express large N limits of these models without quenched randomness.)

Suppose now that the graph \mathcal{G} has a face \mathcal{F}_* of type ab with precisely 2 vertices. As noted earlier, if the degree $\omega(\mathcal{G})$ vanishes, then for any cyclic order \mathcal{J} , the two-manifold $\Sigma_{\mathcal{J}}$ is topologically a

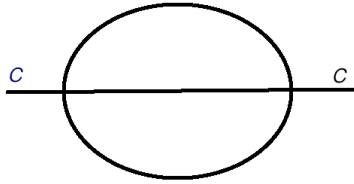


Figure 7: Given a graph \mathcal{G} as in fig. 6(b) that makes a leading contribution to the vacuum amplitude, the “interior” of the face \mathcal{F}_* is a graph that makes a leading contribution to the two-point function. This graph is shown here for the example of fig. 6(b). Gluing together the external lines of this graph, we get another graph \mathcal{G}' , with fewer vertices than \mathcal{G} , that makes a leading order contribution to the vacuum amplitude. In the case shown, this graph is simply the basic one of fig. 4(b).

sphere, and the graph corresponding to \mathcal{J} is planar. Let c be any label in the set $\{0, 1, \dots, D\}$ other than a and b . Consider a cyclic order \mathcal{J} that reads in part $(\dots acb\dots)$ (in other words, part of the sequence is acb). Near \mathcal{F}_* , the planar graph that corresponds to the ordering \mathcal{J} will have to look like part (a) or (b) of fig. 6 (this is essentially fig. 2 of [22]). The two cases differ by whether the two vertices of \mathcal{F}_* are connected by a single propagator with label c (part (a) of the figure) or something more complicated (part (b)).

If the picture looks like fig. 6(a) for all $c \neq a, b$, then the graph \mathcal{G} is precisely the diagram of fig. 4(b), which arises at the first nontrivial step of the iteration that produces the leading graphs of the SYK model.

Suppose instead that the picture looks like fig. 6(b) for some c . Then we finish the argument by an induction on the number n_0 of vertices in the graph \mathcal{G} . Suppose a graph \mathcal{G} that contributes a leading order term to the vacuum amplitude has a face \mathcal{F}_* with two vertices with a local picture that looks like fig. 6(b). Then the “interior” of the face \mathcal{F}_* is a graph (fig. 7) that makes a leading order contribution to the two-point function. If we glue together its two external lines, we get a graph \mathcal{G}' that makes a leading order contribution to the vacuum amplitude. (In the case shown in fig. 7, this will just be again the basic diagram of fig. 4(b).) On the other hand, we can make another graph \mathcal{G}'' that also makes a leading order contribution to the vacuum amplitude by replacing the interior of \mathcal{F}_* by a single propagator (in other words, we modify \mathcal{G} by locally replacing fig. 6(b) by fig. 6(a)). Both \mathcal{G}' and \mathcal{G}'' have fewer vertices than \mathcal{G} so by the inductive hypothesis, we can assume that they are each generated starting with the one-loop vacuum diagram of fig. 4(a) by the inductive procedure of the SYK model. But then the same is true for \mathcal{G} .

To explain part of this more intuitively, we make the following remark. If a graph \mathcal{G} has the property that $g_{\mathcal{J}} = 0$ for some \mathcal{J} , then it is a planar diagram and can be drawn on a two-sphere. But if $\omega(\mathcal{G}) = 0$, then $g_{\mathcal{J}} = 0$ for all \mathcal{J} and there are many different ways to draw \mathcal{G} on a two-sphere. A generic planar diagram can be drawn on a two-sphere in essentially only one way. The inductive procedure that generates the leading order diagrams of the SYK model generates diagrams that

can be drawn on the two-sphere in as many ways as possible. For example, fig. 4(b) is drawn as a planar diagram, and after any permutation of the labels 0,1,2, and 3 it is still planar.

Research supported in part by NSF Grant PHY-1606531. I thank J. Maldacena, D. Stanford, and J. Suh for discussions.

References

- [1] S. Sachdev and Y. Ye, “Gapless Spin Fluid Ground State In A Random, Quantum Heisenberg Magnet,” *Phys. Rev. Lett.* **70** (1993) 3339, arXiv:cond-mat/9212030.
- [2] A. Kitaev, “A Simple Model Of Quantum Holography,” talks at KITP, April 7, 2015 and May 27, 2015, <http://online.kitp.ucsb.edu/online/entangled15/kitaev/>, <http://online.kitp.ucsb.edu/online/entangled15/kitaev2/>.
- [3] S. Sachdev, “Holographic Metals and the Fractionalized Fermi Liquid,” *Phys. Rev. Lett.* **105** (2010) 151602, arXiv:1006.3794.
- [4] S. Sachdev, “Bekenstein-Hawking Entropy And Strange Metals,” *Phys. Rev.* **X5** (2015) 041025, arXiv:1506.05111.
- [5] P. Hosur, X.-L. Qi, D. A. Roberts, and B. Yoshida, “Chaos In Quantum Channels,” *JHEP* **02** (2016) 004, arXiv:1511.04021.
- [6] J. Polchinski and V. Rosenhaus, “The Spectrum in the Sachdev-Ye-Kitaev Model,” arXiv:1601.06768.
- [7] Y.-Z. You, A. W. W. Ludwig, and C. Xu, “Sachdev-Ye-Kitaev Model and Thermalization on the Boundary of Many-Body Localized Fermionic Symmetry Protected Topological States,” arXiv:1602.06964.
- [8] W. Fu and S. Sachdev, “Numerical Study of Fermion and Boson Models with Infinite-Range Random Interactions,” arXiv:1603.05246.
- [9] A. Jevicki, K. Suzuki, and J. Yoon, “Bi-Local Holography in the SYK Model,” arXiv:1603.06246.
- [10] J. Maldacena and D. Stanford, “Comments On The Sachdev-Ye-Kitaev Model,” arXiv:1604.07818.
- [11] D. Bagrets, A. Altland, and A. Kamenev, “Sachdev-Ye-Kitaev Model As Liouville Quantum Mechanics,” *Nucl. Phys.* **B911** (2016) 191-205, arXiv:1607.00694.
- [12] A. Jevicki and K. Suzuki, “Bi-Local Holography In The SYK Model: Perturbations” arXiv:1608.07567.
- [13] Y. Gu, X.-L. Qi, and D. Stanford, “Local Criticality, Diffusion and Chaos in Generalized Sachdev-Ye-Kitaev Models,” arXiv:1609.07832.

- [14] D. J. Gross and V. Rosenhaus, “A Generalization Of Sachdev-Ye-Kitaev,” arXiv:1610.01569.
- [15] A. M. Garcia-Garcia and J. J. M. Verbaarschot, “Spectral and Thermodynamic Properties Of The Sachdev-Ye-Kitaev Model,” arXiv:1610.03816.
- [16] W. Fu, D. Gaiotto, J. Maldacena, and S. Sachdev, “Supersymmetric SYK Models,” arXiv:1610.08917.
- [17] S. Banerjee and E. Altman, “Solvable Model For A Dynamical Quantum Phase Transition From Fast To Slow Scrambling,” arXiv:1610.04619.
- [18] M. Berkooz, P. Narayan, M. Rozali, and J. Simon, “Higher Dimensional Generalizations Of The SYK Model,” arXiv:1610.02422.
- [19] R. Gurau, “The $1/N$ Expansion Of Colored Tensor Models,” *Annales Henri Poincare* **12** (2011) 829-847. arXiv:1011.2726.
- [20] R. Gurau and V. Rivasseau, “The $1/N$ Expansion Of Colored Tensor Models In Arbitrary Dimension,” *Europhys. Lett.* **95** (2011) 50004, arXiv:1101.4182.
- [21] R. Gurau, “The Complete $1/N$ Expansion Of Colored Tensor Models In Arbitrary Dimension,” arXiv:1102.5759.
- [22] V. Bonzom, R. Gurau, A. Riello, and V. Rivasseau, “Critical Behavior Of Colored Tensor Models In The Large N Limit,” *Nucl. Phys.* **B853** (2011) 174-195, *Annales Henri Poincare* **13** (2012) 399-423, arXiv:1105.3122.
- [23] V. Bonzom, R. Gurau, and V. Rivasseau, “Random Tensor Models In The Large N Limit: Uncoloring the Colored Tensor Models,” *Phys. Rev.* **D85** (2012) 084037, arXiv:1202.3637.
- [24] V. Rivasseau, “Random Tensors And Quantum Gravity,” *SIGMA* **12** (2016) 069, arXiv:1603.07270.
- [25] R. Gurau, “Invitation To Random Tensors,” *SIGMA* **12** (2016) 094, arXiv:1609.06439.
- [26] R. Gurau, *Random Tensors* (Oxford University Press, 2016, to be published).
- [27] J. Ambjorn, B. Durhus, and T. Jonsson, “Three-Dimensional Simplicial Quantum Gravity And Generalized Matrix Models,” *Mod. Phys. Lett.* **A06** (1991) 1133.
- [28] M. Gross, “Tensor Models And Simplicial Quantum Gravity In $> 2D$,” *Nucl. Phys.* **B25** (1992) 144-9.
- [29] N. Sasakura, “Tensor Model For Gravity and Orientability of Manifold,” *Mod. Phys. Lett.* **A6** (1991) 2613-2624.
- [30] G. W. Moore, 2015 PiTP Lectures, available at <http://www.physics.rutgers.edu/~gmoore/PiTP-LecturesA.pdf>.